Correlation between the Stereochemistry and Bioactivity in Octahedral Rhodium Prolinato Complexes

Rajaratnam, Rajathees; Martin, Elisabeth K.; Doerr, Markus; Harms, Klaus; Casini, Angela; Meggers, Eric

Published in:
Inorganic Chemistry

DOI:
10.1021/acs.inorgchem.5b01349

Publication date:
2015

Inorganic Chemistry

Article

pubs.acs.org/IC

Correlation between the Stereochemistry and Bioactivity in Octahedral Rhodium Prolinato Complexes

Rajathees Rajaratnam,[†] Elisabeth K. Martin,[†] Markus Dörr,[†] Klaus Harms,[†] Angela Casini,[‡,§] and Eric Meggers*[,†,∥]

[†]Fachbereich Chemie, Philipps-Universität Marburg, Hans-Meerwein-Strasse 4, 35043 Marburg, Germany

[‡]Department of Pharmacokinetics, Toxicology and Targeting, Research Institute of Pharmacy, University of Groningen, Antonius Deusinglaan 1, Groningen 9713 AV, The Netherlands

[§]Cardiff School of Chemistry, University of Cardiff, Park Place, Cardiff CF10 3A, U.K.

[∥]College of Chemistry and Chemical Engineering, Xiamen University, Xiamen 361005, People's Republic of China

Supporting Information

ABSTRACT: Controlling the relative and absolute configuration of octahedral metal complexes constitutes a key challenge that needs to be overcome in order to fully exploit the structural properties of octahedral metal complexes for applications in the fields of catalysis, materials sciences, and life sciences. Herein, we describe the application of a proline-based chiral tridentate ligand to decisively control the coordination mode of an octahedral rhodium(III) complex. We demonstrate the mirror-like relationship of synthesized enantiomers and differences between diastereomers. Further, we demonstrate, using the established pyridocarbazole pharmacophore ligand as part of the organometallic complexes, the importance of the relative and absolute stereochemistry at the metal toward chiral environments like protein kinases. Protein kinase profiling and inhibition data confirm that the proline-based enantiopure rhodium(III) complexes, despite having all of the same constitution, differ strongly in their selectivity properties despite their unmistakably mutual origin. Moreover, two exemplary compounds have been shown to induce different toxic effects in an ex vivo rat liver model.

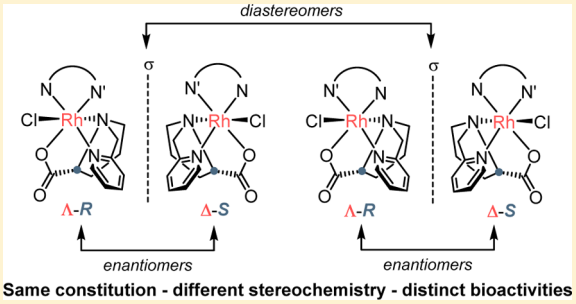

INTRODUCTION

Metals play an important role in medicine and chemical biology.[1] Whereas DNA has been a traditional target for metal complexes, more recent efforts have shifted some attention toward proteins.[2] Our laboratory contributed to this area of research by employing inert metal complexes as structural scaffolds for the design of enzyme inhibitors.[3,4] In this respect, we are convinced that metal complexes featuring an octahedral coordination geometry are particularly powerful templates for achieving selective biomolecular recognition.[5−8] We reported octahedral ruthenium(II),[5] iridium(III),[5,6] and rhodium(III)[7] complexes as selective protein kinase inhibitors, and we demonstrated that some metal complexes outperform most reported organic inhibitors for the same target with respect to binding affinity and kinase selectivity.[9] We attribute these successes to the ability of octahedral coordination geometries to permit the construction of sophisticated globular and often rigid structures based on a combination of rich octahedral stereochemistry and chelation-induced conformational restrictions.[5] The limited conformational flexibility not only provides an entropic advantage reflected in low inhibition constants but also strongly effects the binding specificity. However, the theoretically possible very high structural complexity of octahedral metal complexes, which is maybe comparable with complicated natural products, can only be exploited adequately if synthetic methods exist for control of the relative and absolute stereochemistry in the course of the synthesis of complicated octahedral metal complexes with low symmetry.

An obvious strategy to control the relative and absolute configuration is the use of chiral multidentate ligands. Along these lines, we recently reported a tridentate proline-containing ligand as being part of a cyclometalated rhodium(III) complex, with the pharmacophore ligand 4-phenylpyrrolo[3,4-*c*]-quinoline-1,3(2*H*)-dione leading to enantiopure metal complexes.[7b] This promising initial work inspired us to investigate this chiral ligand in the context of our established metallopyridocarbazole kinase inhibitors (Figure 1). Here we report the synthesis and analysis of four enantiomerically pure stereoisomeric rhodium(III) complexes and investigate their protein kinase binding properties. We demonstrate that the differences in the orientation of the ligand sphere coordinated to the metal center reason the diversity in the selectivity and specificity of the synthesized rhodium(III) pyridocarbazole complexes. Furthermore, preliminary studies of the toxicity of two selected compounds using rat precision cut liver slices

Received: June 16, 2015
Published: August 7, 2015

DOI: 10.1021/acs.inorgchem.5b01349
Inorg. Chem. 2015, 54, 8111−8120

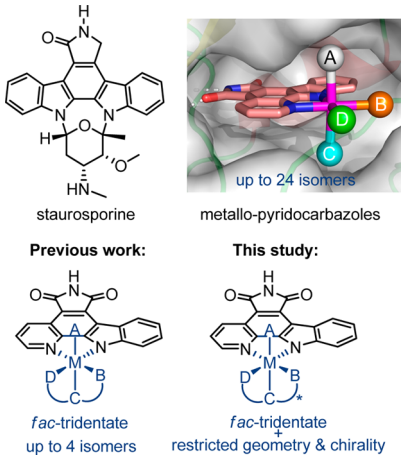

Figure 1. Staurosporine as an inspiration for the design of metallopyridocarbazole complexes as inhibitors of protein kinases.

(PCLSs) were performed ex vivo. Using this technology, all cells remain in their natural environment with maintenance of the original cell−cell and cell−matrix contacts, which is absent in classical 2D cell cultures in vitro. Notably, the technique is an FDA-approved model for drug toxicity and metabolism studies, and it has previously been used for the assessment of toxicity of metal-based compounds like cisplatin (kidney),[10] experimental gold compounds (liver, kidney, and colon),[11] and amino-ferrocen-containing prodrugs (liver).[12]

RESULTS AND DISCUSSION

Synthesis. The rhodium(III) complexes were synthesized in a one-pot reaction under a nitrogen atmosphere in sealed vessels. Accordingly, the pyridocarbazole ligand **1**[13] was reacted first in a sequential addition to a suspension of $RhCl_3{\cdot}3H_2O$ in an ethanol/water mixture at 90 °C for 3 h, followed by addition of the chiral tridentate ligand 1-(pyridin-2-ylmethyl)-pyrrolidine-2-carboxylic acid[7b] with either *R* configuration {(*R*)-**2**} or *S* configuration {(*S*)-**2**} (Scheme 1). Reacting the mixtures at 90 °C for 16 h led to the formation of the two diastereomers Λ-(*R*)-**Rh1** (22%) plus Λ-(*R*)-**Rh2** (15%) starting from (*R*)-**2** and Δ-(*S*)-**Rh1** (24%) plus Δ-(*S*)-**Rh2** (14%) starting from (*S*)-**2**. Note that the absolute configuration of the chiral ligand controls the absolute metal-centered configuration, with the *R* ligand leading to Λ-metal and the *S*-ligand to Δ-metal, so that in the course of each reaction, only two diastereomers are generated. These two diastereomers could be separated by silica gel chromatography with 20:1 to 10:1 methylene chloride/methanol, followed by a preparative thin-layer chromatography (TLC) for each single compound using 15:1 methylene chloride/methanol. The *tert*-butyldimethylsilyl protection group of ligand **1** was observed to be cleaved under the reaction conditions. Additional diastereomers were not detected, which can be rationalized with the restricted possible conformations of the proline-based ligand. The low yields of this reaction may arise from the usage of $RhCl_3{\cdot}3H_2O$ as the starting material. Indeed, rhodium(III) complexes typically react very slowly. Moreover, the labilizing trans effect of chloride is greater than that of the aqua ligand, leading among others to a *fac*-$[RhCl_3(H_2O)_3]$ configuration possessing all aqua ligands in positions opposite to those of the chloride ligands.[14] This *fac*-$[RhCl_3(H_2O)_3]$ configuration is inert to further aquation and thus may also be adverse for ligand exchange by, i.e., ligand **1**, (*R*)-**2**, or (*S*)-**2**, respectively. The

Scheme 1. Synthesis of Nonracemic Rhodium(III) Complexes

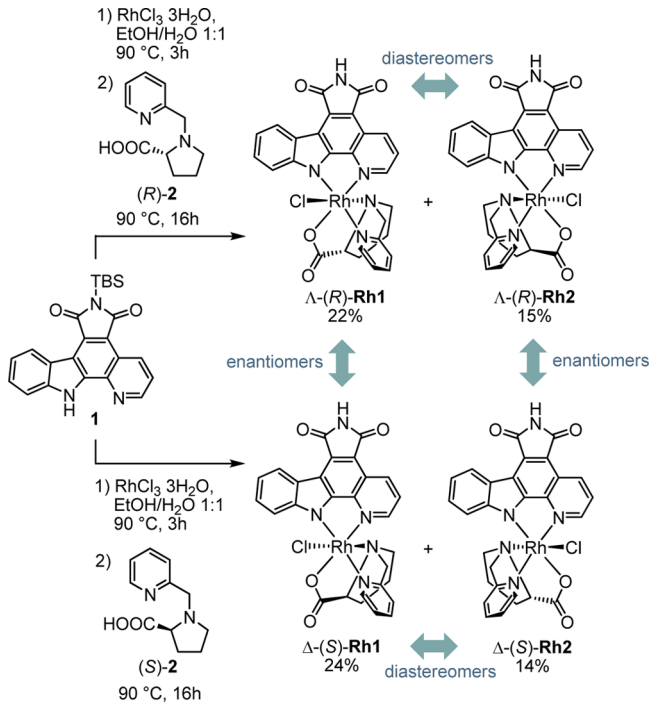

formation of *fac*-$[RhCl_3(H_2O)_3]$ is promoted by free chloride ions, which are inevitably released during the coordination of **1** to the metal center of already reacted $RhCl_3{\cdot}3H_2O$. Therefore, scavenging free chloride ions in solution or preactivating $RhCl_3{\cdot}3H_2O$ into precursors with labilized ligands like $[Rh(C_4H_8S)_{33}Cl_3]$[7a] may improve the product yield. Hence, the general feasibility of enantiopure rhodium(III) prolinato complexes and their biological properties were the main interests of this work; further studies investigating the detailed mechanism of ligand coordination to increase the yields have to be addressed in the future.

Stereochemistry. The absolute stereoconfiguration of Λ-(*R*)-**Rh1** and Δ-(*S*)-**Rh1** was determined via X-ray crystallography (Figure 2). (Detailed crystallographic data are provided in the Supporting Information, SI.) The comparison of the crystal structures of both isomers demonstrates that they are enantiomers and diastereomeric toward Λ-(*R*)-**Rh2** and Δ-(*S*)-**Rh2**. This relationship between the structural isomers was further investigated via circular dichroism (CD) spectroscopy, as shown in Figure 3, revealing the mirror-imaged CD spectra of Λ-(*R*)-**Rh1** compared to Δ-(*S*)-**Rh1** and Λ-(*R*)-**Rh2** compared to Δ-(*S*)-**Rh2**.

Because of the characteristics of the pyridocarbazole and the tridentate ligand used, additional effects can be exploited to distinguish the stereoisomers. For example, the two possible diastereomers Λ-(*R*)-**Rh1** and Λ-(*R*)-**Rh2** can be distinguished easily by correlating their ^{1}H NMR spectra. The hydrogen at position 11 of the pyridocarbazole in Λ-(*R*)-**Rh2** is shifted upfield by 2.1 ppm to a chemical shift of δ = 5.7 ppm compared to Λ-(*R*)-**Rh1** with a chemical shift of δ = 7.8 ppm. This is based on the influence of the aromatic ring current induced by the cis-coordinated pyridine ring (Figure 4). The H-11 proton positioned inside the aromatic ring of the pyridine ring moiety of the tridentate ligand experiences a shielding effect. This effect can only be observed when the pyridine ring of either

DOI: 10.1021/acs.inorgchem.5b01349
Inorg. Chem. 2015, 54, 8111−8120

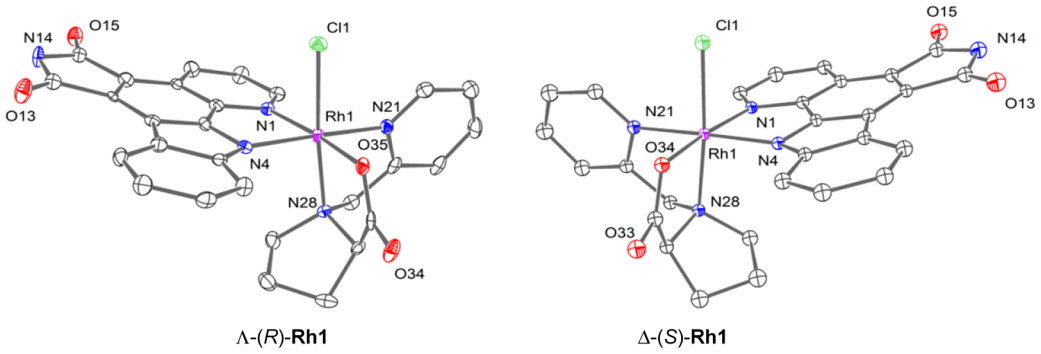

Figure 2. Crystal structures of Λ-(*R*)-**Rh1** and Δ-(*S*)-**Rh1**. Solvent molecules were omitted for clarity. ORTEP drawing with 50% probability of thermal ellipsoids. Selected bond lengths [Å] for Λ-(*R*)-**Rh1**: Rh1−O35 = 2.004(4), Rh1−N21 = 2.032(4), Rh1−N4 = 2.032(4), Rh1−N28 = 2.057(5), Rh1−N1 = 2.071(5), Rh1−Cl1 = 2.3399(16). Selected bond lengths [Å] for Δ-(*S*)-**Rh2**: N1−Rh1 = 2.076(3), N4−Rh1 = 2.036(3), N21−Rh1 = 2.043(3), N28−Rh1 = 2.058(3), O34−Rh1 = 2.004(3), Cl1−Rh1 = 2.3440(11).

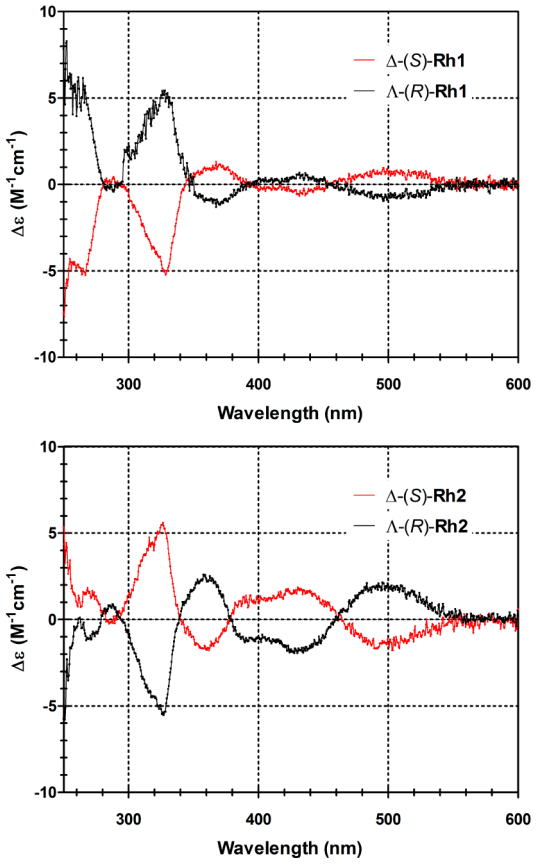

Figure 3. CD spectra of the enantiomerically pure rhodium(III) complexes in DMSO at a concentration of 0.25 mM.

(*R*)-**2** or (*S*)-**2** is coordinated cis and almost perpendicular to the indole moiety of the pyridocarbazole ligand, as is the case for Λ-(*R*)-**Rh2** and Δ-(*S*)-**Rh2**.

Stability. Furthermore, the time-dependent complex stability was determined by solving Λ-(*R*)-**Rh1** and Λ-(*R*)-**Rh2** in dimethyl sulfoxide (DMSO)-d_6/D_2O (9:1) at a final concentration of 5 mM. In addition, to investigate the complex inertness toward free nucleophiles, *β*-mercaptoethanol at a final concentration of 5 mM was added. Indeed, during the investigated time period covering up to 48 h at 25 °C and 24 h at 37 °C, no alterations in the ^{1}H NMR spectra could be observed, confirming the complex stability in the presence of free thiol groups, which are ubiquitous in biological environments (Figure 5).

Kinase Inhibition. To investigate the potential kinase inhibition properties of the four stereoisomeric rhodium complexes, we tested them for their protein kinase binding affinity profile against a large panel of human protein kinases (human kinome).[15] This was accomplished by an active-site-directed affinity screening against 456 human protein kinases.[16] The compounds were screened at 1 *μ*M, and the results for primary screen binding interactions are reported as "percent of control" (POC), where lower numbers indicate stronger interactions, correlating with larger red circles in the dendrogram (Figure 6). Empirical investigations demonstrated that binding constants (K_d) are correlated with such primary screening results, where lower POC values are associated with low K_d values (higher affinity interactions). Moreover, the selectivity score (SS) is a quantitative measure of the compound selectivity. It is calculated by dividing the number of kinases that compounds bind to by the total number of distinct kinases tested, excluding mutant variants. Further, this score value can be calculated for different selectivity levels using POC as a potency threshold, e.g., below 35% or 10%. These SSs clustered in different selectivity score types (SSTs) provide a quantitative method of describing the compound selectivity and allow a facilitated comparison of different compounds among each other.

Depending on the use of L- or D-proline as the starting point for the ligand synthesis of (*S*)-**2** or (*R*)-**2**, the derived complexes differ entirely in their biological properties. Whereas complexes Λ-(*R*)-**Rh2**, Δ-(*S*)-**Rh2**, and Δ-(*S*)-**Rh1** act as kinase inhibitors, complex Λ-(*R*)-**Rh1** is almost ineffective against the tested kinase panel. This is evidenced by the different SSs of the individual compounds. Indeed, Λ-(*R*)-**Rh2** possesses a SS of 0.041 at a SST of 35% and 0.013 at a SST of 10%; Δ-(*S*)-**Rh2** possesses a SS of 0.025 at a SST of 35% and 0.005 at a SST of 10%; Δ-(*S*)-**Rh1** possesses a SS of 0.076 at a SST of 35% and 0.025 at a SST of 10%. In contrast, Λ-(*R*)-**Rh1** did not hit any kinase at the SST levels of 35%, 10%, or even 1% in the tested concentration of 1 *μ*M. None of the four compounds inhibited a kinase in the tested panel at a POC lower than 1%. These remarkable differences of the tested compounds, regarding not only the selectivity across the whole kinome but also the preference to distinct kinase subfamilies addressed by them, indicate the importance of the relative and absolute configuration around the rhodium metal center.

DOI: 10.1021/acs.inorgchem.5b01349
Inorg. Chem. 2015, 54, 8111−8120

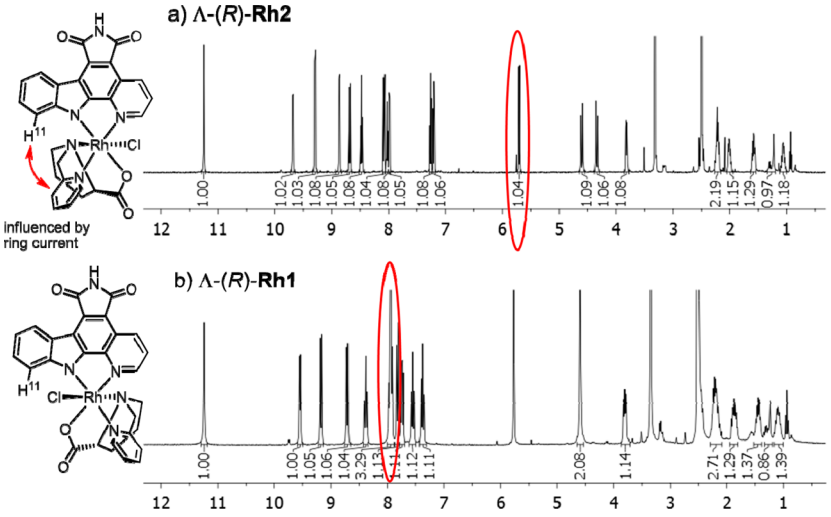

Figure 4. ^{1}H NMR spectra of the diastereomers Λ-(*R*)-**Rh2** and Λ-(*R*)-**Rh1**. The H-11 proton (red circle) of Λ-(*R*)-**Rh2** (a) is upfield-shifted by 2.1 ppm compared to that of Λ-(*R*)-**Rh1** (b) and allows assignment of its relative configuration.

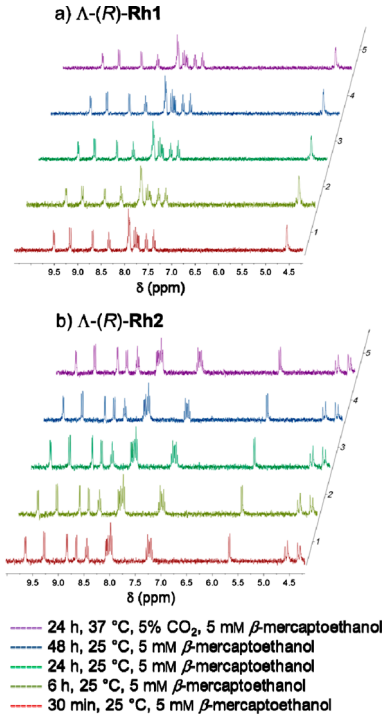

Figure 5. Stability of rhodium complexes in 9:1 DMSO-d_6/D_2O (5 mM) in the presence of β-mercaptoethanol (5 mM). Excerpts of the ^{1}H NMR spectra of the diastereomers Λ-(*R*)-**Rh1** and Λ-(*R*)-**Rh2** are shown after 30 min (red), 6 h (khaki), 24 h (green), and 48 h (blue) at 25 °C as well as 24 h (purple) at 37 °C.

To further verify the primary hits of the kinome profiling, we tested all four compounds in competitive studies using [γ-^{33}P]-adenosine triphosphatase (ATP). Therefore, we selected one target kinase for each compound with a POC lower than 10%. Three kinases were chosen regarding their commercial availability and role in human pathogenesis: Pim-1 (1.8%) addressed by Λ-(*R*)-**Rh2**, Flt-3 (4.9%) addressed by Δ-(*S*)-**Rh2**, and Aurora A (2.4%) addressed by Δ-(*S*)-**Rh1**. For instance, the Pim kinases, covering Pim-1, Pim-2, and Pim-3, prevent cells from apoptosis by phosphorylation of the proapoptotic Bcl-2-associated agonist of cell death (Bad), which abolishes binding with the antiapoptotic protein Bcl-2, leading consequently to increased cell survival.[17a] Moreover, they are involved in cell proliferation through phosphorylation of the cyclin-dependent kinase inhibitors p21.[17b] Because of their digressive expression in several human tumors, they could be important contributors in the pathogenesis of neoplasias including lymphoma, gastric, colorectal, and prostate cancers.[17c−e] The accumulated research results suggest that Flt-3 plays an important role in early hematopoiesis, being involved in proliferation, differentiation, and apoptosis.[18a] Moreover, its increased expression was reported in most cases of acute myeloid leukemia and acute lymphoblastic leukemia.[18b−d] Phosphorylation of Aurora A, beside Aurora B, and Aurora C is related to cell cycle progression, centrosome maturation, and spindle assembly.[19a−c] Furthermore, it is an oncogene and upregulated in several tumor types, and the search for new molecular targets of prostate cancer treatment revealed aurora kinases as promising candidates.[19d−f]

The [γ-^{33}P]-ATP competitive studies confirmed the primary results of the KINOME*scan*. As expected, the target kinases were inhibited profoundly by the compound identified in the kinome profiling (Table 1). Indeed, Λ-(*R*)-**Rh2** inhibited Pim-1 with an IC_{50} of 15 nM, Δ-(*S*)-**Rh2** inhibited Flt-3 with an IC_{50} of 137 nM, and Δ-(*S*)-**Rh1** inhibited Aurora A with an IC_{50} of 121 nM. Further, other structural isomers of the rhodium(III) complexes differ significantly in their IC_{50} values toward the nontarget kinases. For instance, Λ-(*R*)-**Rh1** (1.99 μM), Δ-(*S*)-**Rh2** (1.03 μM), and Δ-(*S*)-**Rh1** (0.88 μM) are significantly less affine toward Pim-1 than the original screening hit Λ-(*R*)-**Rh2**. The same is true for Aurora A [Λ-(*R*)-**Rh1** (164 μM), Λ-(*R*)-**Rh2** (39 μM), and Δ-(*S*)-**Rh2** (35 μM) in contrast to Δ-(*S*)-**Rh1**] as well as for Flt-3 [Λ-(*R*)-**Rh1** (8.47 μM), Λ-(*R*)-**Rh2** (1.2 μM), and Δ-(*S*)-**Rh1** (8.26 μM) in contrast to Δ-(*S*)-**Rh2**]. Moreover, it is worth noting that Λ-(*R*)-**Rh1** is the weakest inhibitor toward all tested kinases. All gathered results of the [γ-^{33}P]-ATP competitive studies are in very good congruence with the results of the kinome profiling and further highlight the importance of the stereochemistry at metal for kinase inhibitors.

However, a detailed comparison between classic organic kinase inhibitors and the rhodium(III) complexes presented here is out of the scope of this work, although the pros and

DOI: 10.1021/acs.inorgchem.5b01349
Inorg. Chem. 2015, 54, 8111−8120

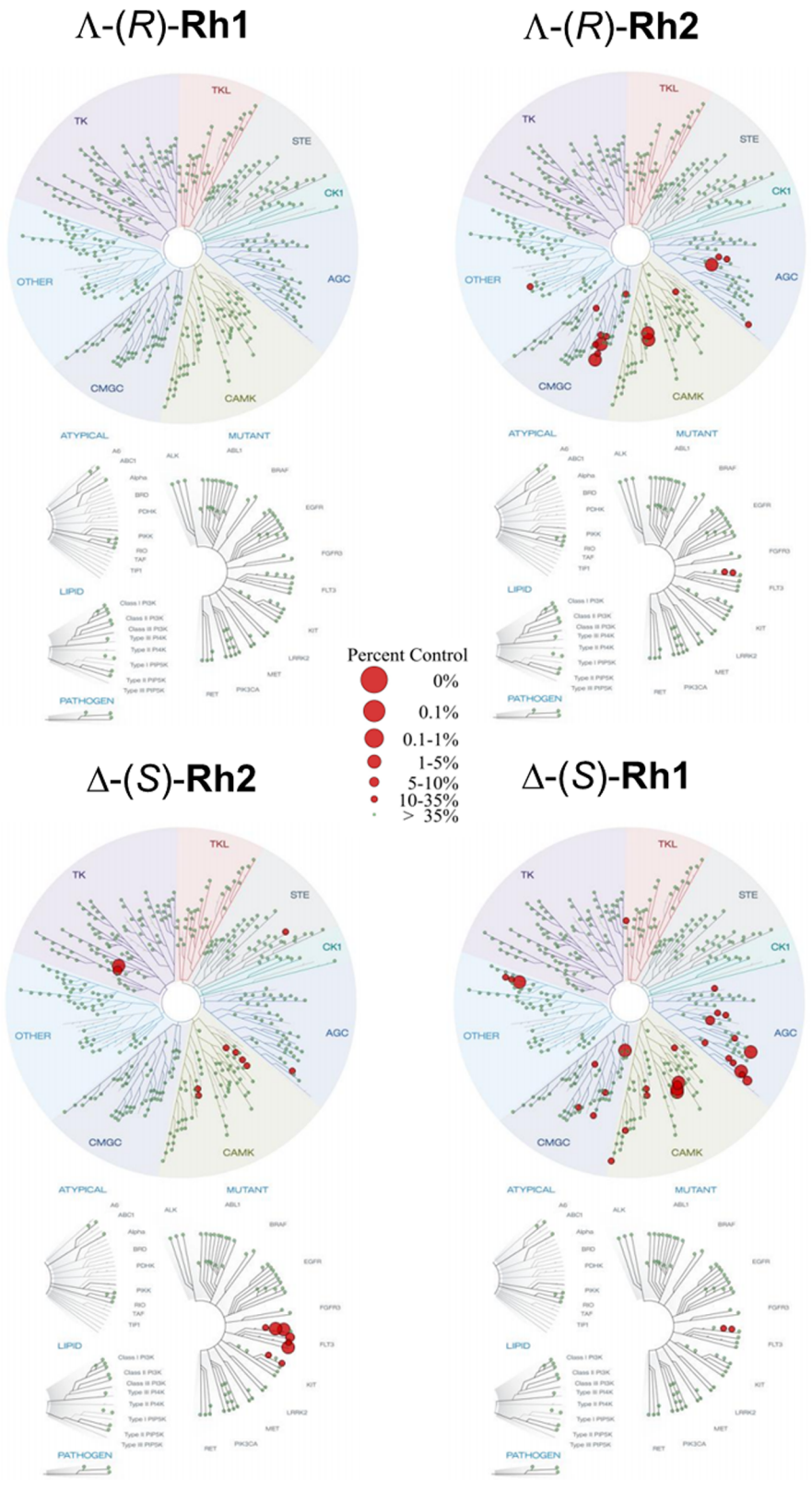

Figure 6. Kinase profiling of Λ-(*R*)-**Rh1**, Λ-(*R*)-**Rh2**, Δ-(*S*)-**Rh2**, and Δ-(*S*)-**Rh1**. All four complexes were tested against 456 human kinases at a concentration of 1 μM by an active-site-directed affinity screening (KINOME*scan*, DiscoveRx). The dendrograms show the remaining activities of the kinases in percentage to the control, depicted as red circles. See the SI for further details.

cons have been discussed before in the literature.[2,5] The Pim kinase family has been described above to possess oncogenic and survival promoting properties.[17] Therefore, targeting members of the Pim kinase family offers potential treatment options, i.e., various leukemias,[17g] mantle cell lymphoma,[17h] and diffuse large B-cell lymphoma.[17i] An actual example of a phase I clinical trial Pim kinase inhibitor is AZD1208 by AstraZeneca.[17j] AZD1208 inhibits the kinase activity of all three

DOI: 10.1021/acs.inorgchem.5b01349
Inorg. Chem. 2015, 54, 8111−8120

Table 1. IC_{50} Data (μM) for Rhodium Kinase Inhibitors[a]

	Aurora A	Pim-1	Flt-3
Λ-(*R*)-**Rh1**	164	2.0	8.5
Δ-(*S*)-**Rh1**	**0.12**	0.88	8.3
Λ-(*R*)-**Rh2**	39	**0.015**	1.2
Δ-(*S*)-**Rh2**	35	1.0	**0.14**

[a] IC_{50} data were obtained by phosphorylation of substrates with [γ-^{33}P]-ATP and 10 μM ATP in the presence of different concentrations of rhodium complexes.

Pim kinases with IC_{50} values of 0.4 nM (Pim-1), 5.0 nM (Pim-2), and 1.9 nM (Pim-3).[17k] Moreover, the organic inhibitor AZD1208 was evaluated in an active-site-directed affinity screening (KINOME*scan*, DiscoveRx) using a panel of 442 kinases, whereas only 16 kinases had a residual activity of less than 50%, including all three Pim kinases.[17k] In comparison, the kinase profiling of Λ-(*R*)-**Rh2** against 456 kinases revealed 23 kinases with a residual activity of less than 50% (see the SI). Moreover, Pim-2 with a POC of exactly 50% was not adequately addressed by Λ-(*R*)-**Rh2** as Pim-1 or Pim-3, both 1.8%. This example shows that Λ-(*R*)-**Rh2** with its low nanomolar IC_{50} value of 15 nM against Pim-1 and its selectivity profile is quite comparable to the literature-known fully organic kinase inhibitors, although the exact selectivity profile inevitably differs. Although differences in the selectivity profiles comparing classic organic inhibitors with metal-based complex inhibitors are likely to be expected, similarities like in the case of Flt-3 confirm a related mode of action. For instance, Flt-3 inhibitors often affect other members of the type III receptor tyrosine kinases including KIT and PDGFR because of their close structural relationship.[18e] This is true for, i.e., SU11248 (Sunitinib, Pfizer),[18f] approved for the treatment of renal cell carcinoma and imatinib-resistant gastrointestinal stromal tumor. Besides also affecting other type III receptor tyrosine kinases like KIT and PDGFR in the kinome profiling, the rhodium(III) inhibitor Δ-(*S*)-**Rh2** possesses a determined IC_{50} value of 137 nM for Flt-3, which is in the same range as the IC_{50} value of SU11248 (250 nM).[18e] In closing, many inhibitors targeting the Aurora kinases have been reported before, and some are evoking increasing focus in clinical trials.[19g−i] For instance, AT9283 developed by Astex Therapeutics is currently in several phase II studies under the Cancer Research UK.[19j] It is a multitarget tyrosine kinase inhibitor, including Aurora A (IC_{50} = 3 nM) and B (IC_{50} = 3 nM), JAK (IC_{50} = 1.2 nM), and T315I Abl (IC_{50} = 4 nM).[19k] In contrast, Δ-(*S*)-**Rh1** inhibits Aurora A in the medium range of an IC_{50} value of 121 nM. Moreover, the kinase profile does not undoubtedly support the mentioned targets of AT9283 as additional targets for Δ-(*S*)-**Rh1** (see the SI).

Despite the short provided framing of the presented rhodium(III) complexes into the context of classic organic kinase inhibitors, it is worth noting that the obtained results reflect just the beginning of enantiopure metal-based kinase inhibitor design. Further improvements of target selectivity and potency are short-term goals achievable by modifying, i.e., the pyridocarbazole pharmacophore ligand **1**,[13c] or attaching additional functional groups to the tridentate ligand (*R*)- or (*S*)-**2**.

Toxicological Studies in PCLSs. Precision-cut tissues are viable explants of the tissue cultured ex vivo with all cell types in their natural environment, providing toxicity results that are expected to be more relevant than those obtained in cell cultures.[20] The tissue is sliced with a reproducible and well-defined thickness, which is small enough to allow sufficient oxygen and nutrient supply to the inner cell layers, ensuring the viability of all cells. Slicing thereby allows a very efficient use of the organ tissue[21] because numerous compounds and conditions can be tested at the same time with only one organ. Precision-cut tissue slices of the liver are frequently used to assess the hepatotoxicity in healthy tissue.[20a,c,d] This is an enormous advantage compared to testing the toxicity in single-cell cultures because drug-induced hepatotoxicity often is a multicellular process involving not only hepatocytes but also other cell types such as Kupffer and stellate cells.[22]

On the basis of their inhibition profile, we selected Λ-(*R*)-**Rh1** and Λ-(*R*)-**Rh2** for hepatotoxicity investigations according to established procedures using rat PCLSs. Λ-(*R*)-**Rh1** was chosen because it is an ineffective kinase inhibitor; therefore, any toxicity should be induced by mechanisms other than kinase inhibition. Λ-(*R*)-**Rh2**, on the other hand, possesses an intermediate kinase selectivity of the remaining three compounds and, in addition, is the diastereomer of Λ-(*R*)-**Rh1**, thereby possessing different physicochemical properties. For hepatotoxicity evaluation, PCLSs were prepared and preincubated for 1 h before exposure to the rhodium-containing complexes, as described in the Experimental Section. Preincubation thereby is necessary to allow the tissue to recover from the cold ischemia and the slicing procedure. The treatment with Λ-(*R*)-**Rh1** and Λ-(*R*)-**Rh2** was performed at three single concentrations of the compounds (1, 10, and 50 μM) with a final DMSO concentration of less than 0.5%, and slices were incubated for 24 h. Afterward, PCLSs were collected, and their viability was determined by measuring their ATP content and normalizing it to their protein content.

Figure 7 reports the viability of the PCLSs upon treatment with different compound concentrations. According to the obtained results, both compounds are not toxic for the slices at a concentration of 1 μM. At 10 μM concentration, some effects on the tissue viability can be observed with respect to the controls, with Λ-(*R*)-**Rh2** markedly more toxic than Λ-(*R*)-**Rh1** (20% and 69% residual viability, respectively). The hepatotoxicity increases with the highest tested compound concentration (50 μM), with Λ-(*R*)-**Rh2** leading to the most pronounced effect (9% residual viability compared to 30%). Notably, the Λ-(*R*)-**Rh1** complex presents reduced hepatotoxicity with respect to cisplatin in the same rat liver model. In fact, at 10 μM the anticancer platinum complex has been observed to induce a reduction of the tissue viability up to 50% (unpublished data from Casini's laboratory). Whether the toxicity of the rhodium

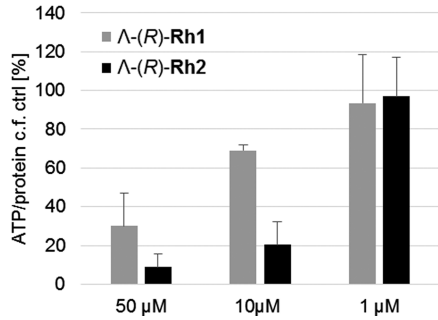

Figure 7. Viability of PCLSs after 24 h of incubation with the two diastereomeric complexes Λ-(*R*)-**Rh1** and Λ-(*R*)-**Rh2** after 1 h of preincubation.

DOI: 10.1021/acs.inorgchem.5b01349
Inorg. Chem. 2015, 54, 8111−8120

complexes is caused by the inhibition of different kinases or of other tissue targets is unclear. However, the Pim-1 kinase, one of the preferred target kinases of the most toxic compound Λ-(*R*)-**Rh2**, is known to be highly expressed in fetal human liver but not in adult tissue,[23] indicating that inhibition of Pim-1 may not be related to the toxicity of the two complexes, at least in humans.

CONCLUSIONS

We here reported our progress in developing structurally complicated and at the same time stereochemically defined metal-based protein kinase inhibitors by employing a tridentate chiral proline-based coordinating ligand. The enantiopure rhodium(III) complexes presented in this work highlight the importance of the access to defined structural isomers regarding molecular recognition with chiral interaction partners like proteins. The remarkable differences in target specificity and affinity are an additional example for the established application of octahedral metal based compounds as kinase inhibitors. Moreover, we paired these benefits with the possibility to investigate single enantiomers, as it is standard for chiral organic compounds in biological context, making organometallic compounds more and more adequate to the requirements of drug-like molecules. Interestingly, different structural isomers may not only possess different kinase inhibition effects, but also different toxicity profiles which may also be due to changes in the overall chemicophysical properties of each isomer. Finally, the scaffold offers plenty of possibilities to introduce additional functional groups in order to improve target specificity and affinity or to enhance pharmacologic properties, as it is the subject of current investigations.

EXPERIMENTAL SECTION

General Information. All reactions were carried out under a nitrogen atmosphere with magnetic stirring. The glass vessels were heated and chilled to ambient temperature at least three times. Solvents were distilled under nitrogen and dried using calcium hydride (CH_3CN, CH_2Cl_2, and $CHCl_3$), sodium/benzophenone (THF), or magnesium shavings (MeOH). All reagents, if not declared otherwise, were purchased from commercial suppliers and used without further purification. Flash column chromatography was performed using silica gel 60 M from Macherey−Nagel (irregular shape, 230−400 mesh, pH 6.8, pore volume = 0.81 mL/g, mean pore size = 66 Å, specific surface = 492 m^2/g, particle size distribution = 0.5% < 25 μm and 1.7% > 71 μm, and water content = 1.6%). ^{1}H NMR and proton-decoupled ^{13}C NMR spectra were measured using a Bruker Avance II 300 (300 MHz) or a Bruker Avance III HD 500 (500 MHz) spectrometer at ambient temperature. The following NMR standards were used. ^{1}H NMR: δ 7.26 ($CDCl_3$), 2.50 ($(CD_3)_2SO$), 2.05 ($(CD_3)_2CO$), 1.94 (CD_3CN). ^{13}C{^{1}H} NMR: δ 77.16 ($CDCl_3$), 39.52 ($(CD_3)_2SO$), 29.84 (residual $(CD_3)_2CO$), 1.32 (CD_3CN). IR spectra were measured using a Bruker Alpha FT-IR spectrophotometer. IR spectra were evaluated using OPUS 6.5 from Bruker Optik GmbH. High-resolution mass spectrometry (HRMS) spectra were measured using a Bruker En Apex Ultra 7.0 TFT-MS instrument using an electrospray ionization technique. CD spectra were recorded on a JASCO J-810 CD spectropolarimeter with cuvettes of 1 mm diameter.

Ligand Synthesis. The pyridocarbazole ligand **1** was synthesized according to established methods.[5,13] The chiral tridentate ligands (*R*)- and (*S*)-**2** were synthesized according to Mollin et al.[7b]

Λ-(*R*)-Rh2 and Λ-(*R*)-Rh1. A suspension of pyridocarbazole **1** (17.6 mg, 44 μmol) and $RhCl_3{\cdot}3H_2O$ (11.5 mg, 44 μmol) in an ethanol/water mixture (1:1, 20 mL) under a nitrogen atmosphere in a sealed vessel was heated to 90 °C for 3 h. During this time, the suspension turned from pale brown to dark red. The reaction mixture was then cooled slightly in order to add (*R*)-1-(pyridin-2-ylmethyl)-pyrrolidine-2-carboxylic acid [(*R*)-**2**; 9.9 mg, 48 μmol]. After the addition of (*R*)-**2**, the reaction further proceeded at 90 °C for 16 h. The reaction mixture was then cooled to ambient temperature, and the solvent was removed in vacuo. The crude material was purified via column chromatography using methylene chloride/methanol (20:1 → 10:1). The separated diastereomers were further purified and concentrated via preparative TLC using methylene chloride/methanol (10:1). The products were obtained as red solids Λ-(*R*)-**Rh2** (4.2 mg, 6.6 μmol, 15%) and Λ-(*R*)-**Rh1** (6.1 mg, 9.7 μmol, 22%). Λ-(*R*)-**Rh2**. ^{1}H NMR [500 MHz, $(CD_3)_2SO$]: δ 11.24 (s, 1H), 9.68 (d, *J* = 5.7 Hz, 1H), 9.30 (dd, *J* = 8.4 and 1.1 Hz, 1H), 8.87 (d, *J* = 5.1 Hz, 1H), 8.68 (dd, *J* = 7.8 and 0.5 Hz, 1H), 8.48 (td, *J* = 7.8 and 1.5 Hz, 1H), 8.08 (dd, *J* = 8.4 and 5.2 Hz, 1H), 8.03 (m, 1H), 7.99 (d, *J* = 7.8 Hz, 1H), 7.28−7.24 (m, 1H), 7.21 (ddd, *J* = 8.4, 7.2, and 1.4 Hz, 1H), 5.70 (d, *J* = 8.2 Hz, 1H), 4.60 (d, *J* = 15.6 Hz, 1H), 4.34 (d, *J* = 15.7 Hz, 1H), 3.81 (dd, *J* = 9.6 and 4.3 Hz, 1H), 2.28−2.15 (m, 2H), 2.00 (dt, *J* = 11.3 and 4.8 Hz, 1H), 1.58 (m, *J* = 11.7 and 5.9 Hz, 1H), 1.35−1.21 (m, 1H), 1.11−1.01 (m, 1H). ^{13}C NMR [126 MHz, $(CD_3)_2SO$]: δ 182.02, 170.59, 170.23, 161.13, 152.62, 152.54, 148.90, 148.74, 142.09, 141.17, 135.24, 131.23, 126.61, 126.27, 124.75, 123.90, 123.47, 121.34, 119.59, 115.08, 114.59, 111.79, 72.91, 70.02, 61.27, 39.52, 30.43, 24.31. IR (film, cm^{-1}): ν 3037, 2075, 1994, 1751, 1703, 1646, 1519, 1482, 1413, 1337, 1296, 1262, 1225, 1132, 1017, 930, 884, 856, 743, 704, 636, 493, 436. HRMS. Calcd for $C_{28}H_{21}ClN_5O_4Rh$ *m*/*z* 652.0229 [(M + Na)$^+$]. Found: *m*/*z* 652.0220 [(M + Na)$^+$]. Λ-(*R*)-**Rh1**. ^{1}H NMR [300 MHz, $(CD_3)_2SO$]: δ 11.24 (s, 1H), 9.54 (d, *J* = 5.5 Hz, 1H), 9.17 (d, *J* = 7.7 Hz, 1H), 8.71 (d, *J* = 7.8 Hz, 1H), 8.38 (m, 1H), 7.99−7.89 (m, 3H), 7.82 (d, *J* = 8.3 Hz, 1H), 7.74 (dd, *J* = 8.4 and 5.3 Hz, 1H), 7.58−7.51 (m, 1H), 7.37 (dd, *J* = 11.1 and 3.9 Hz, 1H), 4.59 (s, 2H), 3.79 (dd, *J* = 9.4 and 4.7 Hz, 1H), 2.29−2.09 (m, 3H), 1.86 (dt, *J* = 11.3 and 5.9 Hz, 1H), 1.44 (dt, *J* = 11.7 and 5.8 Hz, 1H), 1.34−1.19 (m, 1H), 1.10 (dt, *J* = 12.7 and 7.0 Hz, 1H). ^{13}C NMR [101 MHz, $(CD_3)_2SO$]: δ 182.28, 160.15, 152.21, 151.64, 150.36, 149.85, 142.34, 140.72, 134.80, 131.24, 126.56, 126.08, 124.36, 124.17, 123.88, 123.06, 121.09, 119.65, 114.95, 114.87, 114.05, 111.37, 73.50, 69.39, 61.44, 39.52, 30.36, 23.82. IR (film): ν (cm^{-1}) 3045, 2724, 1819, 1750, 1704, 1644, 1519, 1481, 1413, 1336, 1297, 1225, 1134, 1014, 932, 824, 786, 743, 703, 635, 492, 436, 392. HRMS. Calcd for $C_{28}H_{21}ClN_5O_4Rh$: *m*/*z* 652.0229 [(M + Na)$^+$]. Found: *m*/*z* 652.0238 [(M + Na)$^+$].

Δ-(*S*)-Rh2 and Δ-(*S*)-Rh1. Complexes Δ-(*S*)-**Rh1** and Δ-(*S*)-**Rh2** were synthesized similarly to the described method of Λ-(*R*)-**Rh1** and Λ-(*R*)-**Rh2**. The amounts of reactants used were 6-(*tert*-butyldimethylsilyl)pyrido[2,3-*a*]pyrrolo[3,4-*c*]carbazole-5,7-(6*H*,12*H*)-dione (**1**; 17.6 mg, 44 μmol), $RhCl_3{\cdot}3H_2O$ (11.5 mg, 44 μmol), and (*S*)-1-(pyridin-2-ylmethyl)pyrrolidine-2-carboxylic acid [(*S*)-**2**; 9.9 mg, 48 μmol]. The products were obtained as red solids Δ-(*S*)-**Rh2** (3.9 mg, 6.2 μmol, 14%) and Δ-(*S*)-**Rh1** (6.7 mg, 10.6 μmol, 24%). Δ-(*S*)-**Rh2**. ^{1}H NMR [500 MHz, $(CD_3)_2SO$]: δ 11.25 (s, 1H), 9.68 (d, *J* = 5.4 Hz, 1H), 9.30 (d, *J* = 8.3 Hz, 1H), 8.87 (d, *J* = 4.8 Hz, 1H), 8.68 (d, *J* = 7.7 Hz, 1H), 8.48 (dd, *J* = 11.5 and 4.1 Hz, 1H), 8.08 (dd, *J* = 8.3 and 5.2 Hz, 1H), 8.03 (t, *J* = 6.6 Hz, 1H), 7.99 (d, *J* = 7.7 Hz, 1H), 7.26 (t, *J* = 7.4 Hz, 1H), 7.21 (t, *J* = 7.4 Hz, 1H), 5.70 (d, *J* = 8.2 Hz, 1H), 4.60 (d, *J* = 15.8 Hz, 1H), 4.34 (d, *J* = 15.8 Hz, 1H), 3.81 (dd, *J* = 9.3 and 4.0 Hz, 1H), 2.21 (dd, *J* = 17.3 and 10.9 Hz, 2H), 2.04−1.97 (m, 1H), 1.61−1.54 (m, 1H), 1.30−1.21 (m, 1H), 1.11−1.01 (m, 1H). ^{13}C NMR [126 MHz, $(CD_3)_2SO$]: δ 182.02, 170.60, 170.23, 161.13, 152.68, 152.54, 148.90, 148.74, 142.09, 141.17, 135.24, 131.23, 126.61, 126.27, 124.75, 123.90, 123.47, 121.34, 119.59, 115.08, 114.59, 111.79, 72.91, 70.02, 61.27, 39.52, 30.43, 24.31. IR (film, cm^{-1}): ν 3034, 2159, 2096, 1751, 1704, 1646, 1519, 1483, 1413, 1337, 1295, 1262, 1225, 1131, 1015, 930, 828, 784, 744, 705, 636, 527, 491. HRMS. Calcd for $C_{28}H_{21}ClN_5O_4Rh$: *m*/*z* 652.0229 [(M + Na)$^+$]. Found: *m*/*z* 652.0208 [(M + Na)$^+$]. Δ-(*S*)-**Rh1**. ^{1}H NMR [300 MHz, $(CD_3)_2SO$]: δ 11.22 (s, 1H), 9.54 (d, *J* = 5.1 Hz, 1H), 9.18 (dd, *J* = 8.4 and 1.0 Hz, 1H), 8.71 (d, *J* = 7.9 Hz, 1H), 8.38 (td, *J* = 7.7 and 1.5 Hz, 1H), 8.00−7.89 (m, 3H), 7.82 (d, *J* = 8.3 Hz, 1H), 7.74 (dd, *J* = 8.4 and 5.3 Hz, 1H), 7.59−7.50 (m, 1H), 7.41−7.33 (m, 1H), 4.58 (s, 2H), 3.79 (dd, *J* = 9.4 and 4.8 Hz, 1H), 2.25−2.12 (m, 2H), 1.94−1.77 (m, 1H), 1.50−1.37 (m, 1H), 1.31−1.17 (m, 1H), 1.17−0.98 (m, 1H).

DOI: 10.1021/acs.inorgchem.5b01349
Inorg. Chem. 2015, 54, 8111−8120

^{13}C NMR [101 MHz, $(CD_3)_2SO$]: δ 182.29, 160.16, 152.22, 151.65, 150.37, 149.86, 142.45, 142.35, 140.73, 134.81, 131.25, 126.57, 126.09, 124.37, 124.26, 123.90, 123.07, 121.10, 119.66, 114.96, 114.89, 114.01, 73.52, 69.25, 61.45, 39.53, 30.38, 23.83. IR (film, cm^{-1}): ν 3046, 2723, 1818, 1752, 1703, 1647, 1518, 1482, 1414, 1337, 1295, 1224, 1133, 1012, 932, 824, 786, 742, 701, 637, 492, 436. HRMS. Calcd for $C_{28}H_{21}ClN_5O_4Rh$: m/z 652.0229 [$(M + Na)^+$]. Found: m/z 652.0228 [$(M + Na)^+$].

Kinome Profiling and IC_{50} Determination. The protein kinase selectivity profiles of all four rhodium(III) compounds, Λ-(*R*)-**Rh1**, Λ-(*R*)-**Rh2**, Δ-(*S*)-**Rh2**, and Δ-(*S*)-**Rh1**, were determined at a concentration of 1 μM in an active-site-directed affinity screening against 456 human protein kinases (KINOME*scan*, DiscoveRx).[16] General procedure for the determination of IC_{50} values: Various concentrations of the rhodium(III) complexes were incubated at ambient temperature in 20 mM 3-(*N*-morpholino)propanesulfonic acid/sodium hydroxide, 1 mM ethylenediaminetetraacetic acid (EDTA), 0.01% Brij 35, 5% 2-mercaptoethanol, 1 mg/mL bovine serum albumin (BSA), and 10% DMSO (resulting from the inhibitor stock solution) at pH 7.0 in the presence of a kinase substrate for an incubation time of T_1. The reaction was then initiated by adding ATP in a final concentration of 10 μM and approximately 0.1 μCi/μL of [γ-^{33}P]-ATP. Reactions were performed in a total volume of 25 μL. After an incubation time of T_2, the reaction was terminated by spotting 17.5 μL of the reaction mixture on a circular P81 phosphocellulose paper (2.1 cm diameter, Whatman), followed by washing three times with 0.75% phosphoric acid and once with acetone. The dried P81 papers were transferred to scintillation vials and added with 5 mL of scintillation cocktail (purchased from Roth). The counts per minute (CPM) were measured using a Beckmann Coulter LS6500 multi-purpose scintillation counter and corrected by the background CPM. The IC_{50} values were determined in dublicat for each single concentration and compound. The experiments were repeated independently under the same conditions to verify the results. Nonlinear regression and data evaluation were performed using OriginPro 8G (OriginLab). Modifications for the corresponding kinase targets: The amount of Pim-1 used was 0.1 ng/μL, the concentration of the kinase substrate S6 was 50 μm (purchased from MoBiTec), and the incubation times were T_1 = 30 min and T_2 = 30 min. The amount of Aurora A used was 0.13 ng/μL, the concentration of the kinase substrate Kemptide was 250 μM (purchased from Promega), and the incubation times were T_1 = 45 min and T_2 = 45 min. The amount of Flt-3 used was 1 ng/mL, the concentration of Abltide was 100 μM (purchased from Merck Millipore), and incubation times were T_1 = 90 min and T_2 = 90 min. All kinases were purchased from Merck Millipore.

Crystallography. The crystal structures of single crystals of Λ-(*R*)-**Rh1** and Δ-(*S*)-**Rh1** were determined.[24a] The crystals were obtained after dissolution in a methylene chloride/methanol mixture (15:1) and slow evaporation of the solvent at 4 °C for several days. Both compounds crystallized as orthorhombic red plates with an additional methylene chloride molecule. Crystals were measured on a Bruker D8 QUEST area detector diffractometer. The temperature was kept at 100.15 K during data collection using a wavelength of 0.71073 Å. In both cases, the data collection software Bruker APEX II was applied, and the cell refinement and data reduction software *SAINT* (Bruker AXS Inc.) was used.[24b,c] Data were corrected for absorption using the program *SADABS* (Bruker AXS Inc.).[24d] Non-hydrogen atoms were refined anisotropically. Hydrogen atoms were placed on idealized positions and refined using the "riding model". The programs applied for solution and refinement were *SHELXS-97* and *SHELXL-2013*.[24e,f] The absolute structures of Λ-(*R*)-**Rh1** and Δ-(*S*)-**Rh1** were determined.[24g]

Preparation of Rat PCLS and Toxicity Studies ex Vivo. Liver for the preparation of PCLSs was obtained from male Wistar rats (HsdCpb:WU, Harlan Laboratories) weighing 300−350 g. The rats were housed on a 12 h light/dark cycle in a temperature- and humidity-controlled room with food (Harlan chow no. 2018, Harlan Laboratories) and tap water ad libitum. The animals were allowed to acclimatize for at least 7 days before experimentation. The experimental protocols were approved by the Animal Ethical Committee of the University of Groningen and performed according to strict governmental and international guidelines. The organ was excised under 5% isofluorane/95% O_2 anesthesia and placed into an ice-cold University of Wisconsin organ preservation solution. PCLSs were prepared as previously described.[21] The viability of rat PCLS after 24 h of incubation with Λ-(*R*)-**Rh1** or Λ-(*R*)-**Rh2** and 0, 1, and 24 + 1 h of control was determined via the ATP content of the PCLS, which was measured according to a method described in the literature.[21] Briefly, after the designated incubation time, the slices were collected individually in 1 mL of 70% ethanol containing 2 mM EDTA (pH 10.9), quick-frozen in liquid nitrogen, and stored at −80 °C. The samples were thawed on ice, homogenized for 45 s using a Mini-BeadBeater (BioSpec Products), and centrifuged for 5 min at 13000 rpm and 4 °C. The supernatant was separated from the pellet and diluted with Tris HCl (0.1 M) containing 2 mM EDTA (pH 7.8). The ATP content of this dilution was measured in a black 96-well microplate format using the ATP Bioluminescence Assay Kit CLS II (Roche Diagnostics GmbH, Mannheim, Germany) and a LumiCount microplate luminometer (Packard, model BL10001). The ATP content was then calculated by comparison to a standard calibration curve. The remaining pellet was dried at room temperature for at least 72 h, dissolved in 200 μL of NaOH (5 M), and incubated at 37 °C in a shaking water bath for 30 min. The solution was diluted with 800 μL of water (final NaOH concentration of 1M) and homogenized again for 40 s with a Mini-BeadBeater. The protein content was then determined using a Bio-Rad DC Protein Assay (Bio-Rad Laboratories) in a 96-well microplate assay format compared to a BSA calibration curve. The ATP content of the slice was than normalized to the protein content (pmol of ATP/μg of protein) and expressed as a value relative to the 24 h control tissue. Obtained values are the mean of at least two (1 μM) or three (10 and 50 μM) independent experiments.

■ ASSOCIATED CONTENT

Supporting Information

The Supporting Information is available free of charge on the ACS Publications website at DOI: 10.1021/acs.inorgchem.5b01349.

Detailed kinase profiling data of Λ-(*R*)-**Rh1**, Λ-(*R*)-**Rh2**, Δ-(*S*)-**Rh1**, and Δ-(*S*)-**Rh2**, detailed IC_{50} graphs, crystallographic data of Λ-(*R*)-**Rh1** and Δ-(*S*)-**Rh1**, and additional references (PDF)

X-ray crystallographic data of Λ-(*R*)-**Rh1** and Δ-(*S*)-**Rh1** (CIF)

■ AUTHOR INFORMATION

Corresponding Author

*E-mail: meggers@chemie.uni-marburg.de.

Notes

The authors declare no competing financial interest.

■ ACKNOWLEDGMENTS

This work was supported by a LOEWE Research Cluster (SynChemBio) of the Federal State of Hesse and the U.S. National Institutes of Health (Grant CA025874). The authors acknowledge the contribution of the COST Action CM1105.

■ REFERENCES

(1) For metal complexes in the life sciences, see: (a) Guo, Z.; Sadler, P. J. *Angew. Chem., Int. Ed.* **1999**, *38*, 1512−1531. (b) Fish, R. H.; Jaouen, G. *Organometallics* **2003**, *22*, 2166−2177. (c) Alberto, R. *J. Organomet. Chem.* **2007**, *692*, 1179−1186. (d) Zeglis, B. M.; Pierre, V. C.; Barton, J. K. *Chem. Commun.* **2007**, 4565−4579. (e) Hambley, T. W. *Science* **2007**, *318*, 1392−1393. (f) Levina, A.; Mitra, A.; Lay, P. A. *Metallomics* **2009**, *1*, 458−470. (g) Keene, F. R.; Smith, J. A.; Collins, J. G. *Coord. Chem. Rev.* **2009**, *253*, 2021−2035. (h) Haas, K. L.; Franz, K.

DOI: 10.1021/acs.inorgchem.5b01349
Inorg. Chem. 2015, 54, 8111−8120

J. *Chem. Rev.* **2009**, *109*, 4921−4960. (i) Schatzschneider, U. *Eur. J. Inorg. Chem.* **2010**, *2010*, 1451−1467. (j) Gasser, G.; Ott, I.; Metzler-Nolte, N. *J. Med. Chem.* **2011**, *54*, 3−25. (k) Hillard, E. A.; Jaouen, G. *Organometallics* **2011**, *30*, 20−27. (l) Schatzschneider, U. *Inorg. Chim. Acta* **2011**, *374*, 19−23. (m) Salassa, L. *Eur. J. Inorg. Chem.* **2011**, *2011*, 4931−4947. (n) Bergamo, A.; Sava, G. *Dalton Trans.* **2011**, *40*, 7817−7823. (o) Che, C.-M.; Sun, R. W.-Y. *Chem. Commun.* **2011**, *47*, 9554−9560. (p) Patra, M.; Gasser, G. *ChemBioChem* **2012**, *13*, 1232−1252. (q) Hartinger, C. G.; Metzler-Nolte, N.; Dyson, P. J. *Organometallics* **2012**, *31*, 5677−5685. (r) Lo, K. K.-W.; Choi, A. W.-T.; Law, W. H.-T. *Dalton Trans.* **2012**, *41*, 6021−6047. (s) Oehninger, L.; Rubbiani, R.; Ott, I. *Dalton Trans.* **2013**, *42*, 3269−3284. (t) Ma, D.-L.; He, H.-Z.; Leung, K.-H.; Chan, D. S.-H.; Leung, C.-H. *Angew. Chem., Int. Ed.* **2013**, *52*, 7666−7682. (u) Mjos, K. D.; Orvig, C. *Chem. Rev.* **2014**, *114*, 4540−4563.

(2) For targeting metal complexes to proteins, see: (a) Meggers, E. *Chem. Commun.* **2009**, 1001−1010. (b) Davies, C. L.; Dux, E. L.; Duhme-Klair, A.-K. *Dalton Trans.* **2009**, 10141−10154. (c) Che, C.-M.; Siu, F.-M. *Curr. Opin. Chem. Biol.* **2010**, *14*, 255−261. (d) Kilpin, K. J.; Dyson, P. J. *Chem. Sci.* **2013**, *4*, 1410−1419. (e) Leung, C.-H.; He, H.-Z.; Liu, L.-J.; Wang, M.; Chan, D. S.-H.; Ma, D.-L. *Coord. Chem. Rev.* **2013**, *257*, 3139−3151. (f) De Almeida, A. B.; Oliveira, L.; Correia, J. D. G.; Soveral, G.; Casini, A. *Coord. Chem. Rev.* **2013**, *257*, 2689−2704. (g) Barry, N. P. E.; Sadler, P. J. *Chem. Commun.* **2013**, *49*, 5106−5131. (h) Dörr, M.; Meggers, E. *Curr. Opin. Chem. Biol.* **2014**, *19*, 76−81.

(3) For Francis P. Dwyer's pioneering work on this topic, see: Kilah, N. L.; Meggers, E. *Aust. J. Chem.* **2012**, *65*, 1325−1332.

(4) For our early work, see: Meggers, E.; Atilla-Gokcumen, G. E.; Bregman, H.; Maksimoska, J.; Mulcahy, S. P.; Pagano, N.; Williams, D. S. *Synlett* **2007**, *2007*, 1177−1189.

(5) (a) Maksimoska, J.; Feng, L.; Harms, K.; Yi, C.; Kissil, J.; Marmorstein, R.; Meggers, E. *J. Am. Chem. Soc.* **2008**, *130*, 15764−15765. (b) Feng, L.; Geisselbrecht, Y.; Blanck, S.; Wilbuer, A.; Atilla-Gokcumen, G. E.; Filippakopoulos, P.; Kräling, K.; Celik, M. A.; Harms, K.; Maksimoska, J.; Marmorstein, R.; Frenking, G.; Knapp, S.; Essen, L.-O.; Meggers, E. *J. Am. Chem. Soc.* **2011**, *133*, 5976−5986. (c) Blanck, S.; Maksimoska, J.; Baumeister, J.; Harms, K.; Marmorstein, R.; Meggers, E. *Angew. Chem., Int. Ed.* **2012**, *51*, 5244−5246. (d) Mulcahy, S. P.; Meggers, E. *Top. Organomet. Chem.* **2010**, *32*, 141−153.

(6) (a) Wilbuer, A.; Vlecken, D. H.; Schmitz, D. J.; Kräling, K.; Harms, K.; Bagowski, C. P.; Meggers, E. *Angew. Chem., Int. Ed.* **2010**, *49*, 3839−3842. (b) Kunick, C.; Ott, I. *Angew. Chem., Int. Ed.* **2010**, *49*, 5226−5227. (c) Göbel, P.; Ritterbusch, F.; Helms, M.; Bischof, M.; Harms, K.; Jung, M.; Meggers, E. *Eur. J. Inorg. Chem.* **2015**, *2015*, 1654−1659.

(7) (a) Dieckmann, S.; Riedel, R.; Harms, K.; Meggers, E. *Eur. J. Inorg. Chem.* **2012**, *2012*, 813−821. (b) Mollin, S.; Blanck, S.; Harms, K.; Meggers, E. *Inorg. Chim. Acta* **2012**, *393*, 261−268. (c) Mollin, S.; Riedel, R.; Harms, K.; Meggers, E. *J. Inorg. Biochem.* **2015**, *148*, 11−21.

(8) (a) Leung, C.-H.; Zhong, H.-J.; Yang, H.; Cheng, Z.; Chan, D. S.-H.; Ma, V. P.-Y.; Abagyan, R.; Wong, C.-Y.; Ma, D.-L. *Angew. Chem., Int. Ed.* **2012**, *51*, 9010−9014. (b) Zhong, H.; Yang, H.; Chan, D. S.; Leung, C.; Wang, H.; Ma, D.-L. *PLoS One* **2012**, *7*, e49574. (c) Oliveira, B. L.; Moreira, I. S.; Fernandes, P. A.; Ramos, M. J.; Santos, I.; Correia, J. D. G. *J. Mol. Graphics Modell.* **2013**, *45*, 13−25. (d) Zhong, H.-J.; Leung, K.-H.; Liu, L.-J.; Lu, L.; Chan, D. S.-H.; Leung, C.-H.; Ma, D.-L. *ChemPlusChem* **2014**, *79*, 508−511. (e) Ma, D.-L.; Liu, L.-J.; Leung, K.-H.; Chen, Y.-T.; Zhong, H.-J.; Chan, D. S.-H.; Wang, H.-M. D.; Leung, C.-H. *Angew. Chem., Int. Ed.* **2014**, *53*, 9178−9182. (f) Liu, L.-J.; Lin, S.; Chan, D. S.-H.; Vong, C. T.; Hoi, P. M.; Wong, C.-Y.; Ma, D.-L.; Leung, C.-H. *J. Inorg. Biochem.* **2014**, *140*, 23−28. (g) Leung, C.-H.; Liu, L.-J.; Lu, L.; He, B.; Kwong, D. W. J.; Wong, C.-Y.; Ma, D.-L. *Chem. Commun.* **2015**, *51*, 3973−3976. (h) Oliveira, B. L.; Morais, M.; Mendes, F.; Moreira, I. S.; Cordeiro, C.; Fernandes, P. A.; Ramos, M. J.; Alberto, R.; Santos, I.; Correia, J. D. G. *Chem. Biol. Drug Des.* **2015**, DOI: 10.1111/cbdd.12575.

(9) For metal-containing protein kinase inhibitors from other groups, see: (a) Spencer, J.; Mendham, A. P.; Kotha, A. K.; Richardson, S. C. W.; Hillard, E. A.; Jaouen, G.; Male, L.; Hursthouse, M. B. *Dalton Trans.* **2009**, 918−921. (b) Biersack, B.; Zoldakova, M.; Effenberger, K.; Schobert, R. *Eur. J. Med. Chem.* **2010**, *45*, 1972−1975. (c) Spencer, J.; Amin, J.; Callear, S. K.; Tizzard, G. J.; Coles, S. J.; Coxhead, P.; Guille, M. *Metallomics* **2011**, *3*, 600−608. (d) Ginzinger, W.; Mühlgassner, G.; Arion, V. B.; Jakupec, M. A.; Roller, A.; Galanski, M.; Reithofer, M.; Berger, W.; Keppler, B. K. *J. Med. Chem.* **2012**, *55*, 3398−3413. (e) Amin, J.; Chuckowree, I.; Tizzard, G. J.; Coles, S. J.; Wang, M.; Bingham, J. P.; Hartley, J. A.; Spencer, J. *Organometallics* **2013**, *32*, 509−513. (f) Amin, J.; Chuckowree, I. S.; Wang, M.; Tizzard, G. J.; Coles, S. J.; Spencer, J. *Organometallics* **2013**, *32*, 5818−5825.

(10) Vickers, A. E. M.; Rose, K.; Fisher, R.; Saulnier, M.; Sahota, P.; Bentley, P. *Toxicol. Pathol.* **2004**, *32*, 577−590.

(11) Bertrand, B.; Stefan, L.; Pirrotta, M.; Monchaud, D.; Bodio, E.; Richard, P.; Le Gendre, P.; Warmerdam, E.; de Jager, M. H.; Groothuis, G. M. M.; et al. *Inorg. Chem.* **2014**, *53*, 2296−303.

(12) Daum, S.; Chekhun, V. F.; Todor, I. N.; Lukianova, N. Y.; Shvets, Y. V.; Sellner, L.; Putzker, K.; Lewis, J.; Zenz, T.; de Graaf, I. A. M.; et al. *J. Med. Chem.* **2015**, *58*, 2015−2024.

(13) (a) Bregman, H.; Williams, D. S.; Atilla, G. E.; Carroll, P. J.; Meggers, E. *J. Am. Chem. Soc.* **2004**, *126*, 13594−13595. (b) Bregman, H.; Williams, D. S.; Meggers, E. *Synthesis* **2005**, *9*, 1521−1527. (c) Pagano, N.; Maksimoska, J.; Bregman, H.; Williams, D. S.; Webster, R. D.; Xue, F.; Meggers, E. *Org. Biomol. Chem.* **2007**, *5*, 1218−1227.

(14) Jardine, F. H. *Encyclopedia of Inorganic Chemistry*; John Wiley & Sons, Ltd.: New York, 2006.

(15) Manning, G.; Whyte, D. B.; Martinez, R.; Hunter, T.; Sudarsanam, S. *Science* **2002**, *298*, 1912−1934.

(16) (a) Fabian, M. A.; Biggs, W. H.; Treiber, D. K.; Atteridge, C. E.; Azimioara, M. D.; Benedetti, M. G.; et al. *Nat. Biotechnol.* **2005**, *23*, 329−336. (b) Karaman, M. W.; Herrgard, S.; Treiber, D. K.; Gallant, P.; Atteridge, C. E.; Campbell, B. T.; Chan, K. W.; Ciceri, P.; Davis, M. I.; Edeen, P. T.; et al. *Nat. Biotechnol.* **2008**, *26*, 127−132.

(17) (a) Macdonald, A.; Campbell, D.; Toth, R.; McLauchlan, H.; Hastie, C. J.; Arthur, J. S. *BMC Cell Biol.* **2006**, *7*, 1. (b) Morishita, D.; Katayama, R.; Sekimizu, K.; Tsuruo, T.; Fujita, N. *Cancer Res.* **2008**, *68*, 5076−5085. (c) Wingett, D.; Long, A.; Kelleher, D.; Magnuson, N. S. *J. Immunol.* **1996**, *156*, 549−557. (d) Cibull, T. L.; Jones, T. D.; Li, L.; Eble, J. N.; Baldridge, L. A.; Malott, S. R.; Luo, Y.; Cheng, L. *J. Clin. Pathol.* **2006**, *59*, 285−288. (e) Shah, N.; Pang, B.; Yeoh, K.-G.; Thorn, S.; Chen, C. S.; Lilly, M. B.; Salto-Tellez, M. *Eur. J. Cancer* **2008**, *44*, 2144−2151. (f) Merkel, A. L.; Meggers, E.; Ocker, M. *Expert Opin. Invest. Drugs* **2012**, *21*, 425−436. (g) Amson, R.; Sigaux, F.; Przedborski, S.; Flandrin, G.; Givol, D.; Telerman, A. *Proc. Natl. Acad. Sci. U. S. A.* **1989**, *86*, 8857−61. (h) Hsi, E. D.; Jung, S.-H.; Lai, R.; Johnson, J. L.; Cook, J. R.; Jones, D.; Devos, S.; Cheson, B. D.; Damon, L. E.; Said, J. *Leuk. Lymphoma* **2008**, *49*, 2081−2090. (i) Mahadevan, D.; Spier, C.; Della Croce, K.; Miller, S.; George, B.; Riley, C.; Warner, S.; Grogan, T. M.; Miller, T. P. *Mol. Cancer Ther.* **2005**, *4*, 1867−1879. (j) Dakin, L. A.; Block, M. H.; Chen, H.; Code, E.; Dowling, J. E.; Feng, X.; Ferguson, A. D.; Green, I.; Hird, A. W.; Howard, T.; Keeton, E. K.; Lamb, M. L.; Lyne, P. D.; Pollard, H.; Read, J.; Wu, A. J.; Zhang, T.; Zheng, X. *Bioorg. Med. Chem. Lett.* **2012**, *22*, 4599−4604. (k) Keeton, E. K.; McEachern, K.; Dillman, K. S.; Palakurthi, S.; Cao, Y.; Grondine, M. R.; Kaur, S.; Wang, S.; Chen, Y.; Wu, A.; Shen, M.; Gibbons, F. D.; Lamb, M. L.; Zheng, X.; Stone, R. M.; DeAngelo, D. J.; Platanias, L. C.; Dakin, L. A.; Chen, H.; Lyne, P. D.; Huszar, D. *Blood* **2014**, *123*, 905−913.

(18) (a) Stirewalt, D. L.; Radich, J. P. *Nat. Rev. Cancer* **2003**, *3*, 650−665. (b) Drexler, H. G. *Leukemia* **1996**, *10*, 588−599. (c) Abu-Duhier, F. M.; Goodeve, A. C.; Wilson, G. A.; Care, R. S.; Peake, I. R.; Reilly, J. T. *Br. J. Haematol.* **2001**, *113*, 983−988. (d) Ravandi, F.; Kantarjian, H.; Faderl, S.; Garcia-Manero, G.; O'Brien, S.; Koller, C.; Pierce, S.; Brandt, M.; Kennedy, D.; Cortes, J.; et al. *Leuk. Res.* **2010**, *34*, 752−756. (e) van der Geer, P.; Hunter, T.; Lindberg, R. A. *Annu. Rev. Cell*

DOI: 10.1021/acs.inorgchem.5b01349
Inorg. Chem. 2015, 54, 8111−8120

Biol. **1994**, *10*, 251−337. (f) O'Farrell, A.-M.; Abrams, T. J.; Yuen, H. A.; Ngai, T. J.; Louie, S. G.; Yee, K. W. H.; Wong, L. M.; Hong, W.; Lee, L. B.; Town, A. *Blood* **2003**, *101*, 3597−3605.
(19) (a) Vader, G.; Lens, S. M. A. *Biochim. Biophys. Acta, Rev. Cancer* **2008**, *1786*, 60−72. (b) Carmena, M.; Earnshaw, W. C. *Nat. Rev. Mol. Cell Biol.* **2003**, *4*, 842−854. (c) Sardon, T.; Peset, I.; Petrova, B.; Vernos, I. *EMBO J.* **2008**, *27*, 2567−2579. (d) Malumbres, M.; Pérez de Castro, I. *Expert Opin. Ther. Targets* **2014**, *18*, 1377−1393. (e) Hilton, J. F.; Shapiro, G. I.; Hospital, W.; Medical, H. 2015, *32*, 57−59. (f) Nikonova, A.; Astsaturov, I.; Serebriiskii, I.; Dunbrack, R., Jr.; Golemis, E. *Cell. Mol. Life Sci.* **2013**, *70*, 661−687. (g) Kollareddy, M.; Zheleva, D.; Dzubak, P.; Brahmkshatriya, P. S.; Lepsik, M.; Hajduch, M. *Invest. New Drugs* **2012**, *30*, 2411−2432. (h) Dar, A. A.; Goff, L. W.; Majid, S.; Berlin, J.; El-Rifai, W. *Mol. Cancer Ther.* **2010**, *9*, 268−278. (i) Goldenson, B.; Crispino, J. D. *Oncogene* **2015**, *34*, 537−545. (j) Ritchie, J. W. A.; Williams, R. J. *Drug Discovery Today* **2015**, DOI: 10.1016/j.drudis.2015.03.006. (k) Howard, S.; Berdini, V.; Boulstridge, J. A.; Carr, M. G.; Cross, D. M.; Curry, J.; Devine, L. A.; Early, T. R.; Fazal, L.; Gill, A. L. *J. Med. Chem.* **2008**, *52*, 379−388.
(20) For the use of precision-cut tissue slices as in vitro models of organs, see: (a) Parrish, A. R.; Gandolfi, A. J.; Brendel, K. *Life Sci.* **1995**, *57*, 1887−1901. (b) Gandolfi, A. J.; Wijeweera, J.; Brendel, K. *Toxicol. Pathol.* **1996**, *24*, 58−61. (c) Olinga, P.; Meijer, D. K. F.; Slooff, M. J. H.; Groothuis, G. M. M. *Toxicol. In Vitro* **1997**, *12*, 77−100. (d) Vickers, A. E. M.; Fisher, R. L. *Expert Opin. Drug Metab. Toxicol.* **2005**, *1*, 687−699. (e) De Graaf, I. A.; Groothuis, G. M.; Olinga, P. *Expert Opin. Drug Metab. Toxicol.* **2007**, *3*, 879−898. (f) Olinga, P.; Schuppan, D. *J. Hepatol.* **2013**, *58*, 1252−1253. (g) Fisher, R. L.; Vickers, A. E. M. *Xenobiotica* **2013**, *43*, 8−14. (h) Koch, A.; Saran, S.; Tran, D. D. H.; Klebba-Färber, S.; Thiesler, H.; Sewald, K.; Schindler, S.; Braun, A.; Klopfleisch, R.; Tamura, T. *Cell Commun. Signaling* **2014**, *12*, 73.
(21) De Graaf, I. A. M.; Olinga, P.; de Jager, M. H.; Merema, M. T.; de Kanter, R.; van de Kerkhof, E. G.; Groothuis, G. M. M. *Nat. Protoc.* **2010**, *5*, 1540−1551.
(22) Elferink, M. G. L.; Olinga, P.; Draaisma, A. L.; Merema, M. T.; Bauerschmidt, S.; Polman, J.; Schoonen, W. G.; Groothuis, G. M. M. *Toxicol. Appl. Pharmacol.* **2008**, *229*, 300−309.
(23) Amson, R.; Sigaux, F.; Przedborski, S.; Flandrin, G.; Givol, D.; Telerman, A. *Proc. Natl. Acad. Sci. U. S. A.* **1989**, *86*, 8857−8861.
(24) (a) Brandenburg, K. *Diamond—Crystal and Molecular Structure Visualization*; Crystal Impact, Dr. H. Putz & Dr. K. Brandenburg GbR: Bonn, Germany, 2014. (b) *APEX2*; Bruker AXS Inc.: Madison, WI, 2014. (c) *SAINT*; Bruker AXS Inc.: Madison, WI, 2013. (d) *SADABS*; Bruker AXS Inc.: Madison, WI, 2014. (e) Sheldrick, G. M. *Acta Crystallogr., Sect. A: Found. Crystallogr.* **2008**, *64*, 112−122. (f) Sheldrick, G. M. *SHELXL*; Universität Göttingen: Göttingen, Germany, 2014. (g) Parsons, S.; Flack, H. D.; Wagner, T. *Acta Crystallogr., Sect. B: Struct. Sci., Cryst. Eng. Mater.* **2013**, *69*, 249−259.

DOI: 10.1021/acs.inorgchem.5b01349
Inorg. Chem. 2015, 54, 8111−8120